Inorganic Chemistry

Article

pubs.acs.org/IC

Noninnocently Behaving Bridging Anions of the Widely Distributed Antioxidant Ellagic Acid in Diruthenium Complexes

Abhishek Mandal,[†] Anita Grupp,[§] Brigitte Schwederski,[§] Wolfgang Kaim,*[,§] and Goutam Kumar Lahiri*[,†]

[†]Department of Chemistry, Indian Institute of Technology Bombay, Powai, Mumbai-400076, India

[§]Institut für Anorganische Chemie, Universität Stuttgart, Pfaffenwaldring 55, D-70550 Stuttgart, Germany

Supporting Information

ABSTRACT: Dinuclear compounds $[L_2Ru(\mu\text{-}E)RuL_2]^n$ where L is acetylacetonate ($acac^-$, 2,4-pentanedionate), 2,2′-bipyridine (bpy), or 2-phenylazopyridine (pap) and EH_4 is ellagic acid, an antioxidative bis-catechol natural product, were studied by voltammetric and spectroelectrochemical techniques (UV−vis−NIR and electron paramagnetic resonance (EPR)). The electronic structures of the isolated forms $(NBu_4)_2[(acac)_2Ru(\mu\text{-}E)Ru(acac)_2]$ ($(NBu_4)_2[\mathbf{1}]$), $[(bpy)_2Ru(\mu\text{-}E)Ru(bpy)_2]ClO_4$ ($[\mathbf{2}]ClO_4$), and $[(pap)_2Ru(\mu\text{-}E)Ru(pap)_2]$ ($[\mathbf{3}]$) were characterized by density functional theory (DFT) in conjunction with EPR and UV−vis−NIR measurements. The crystal structure of $(NBu_4)_2[\mathbf{1}]$ revealed the *meso* form and a largely planar Ru(μ-E)Ru center. Several additional charge states of the compounds were electrochemically accessible and were identified mostly as complexes with noninnocently behaving $pap^{0/\bullet-}$ or bridging ellagate (E^{n-}) anions (n = 2, 3, 4) but not as mixed-valence intermediates. The free anions E^{n-}, n = 1−4, were calculated by time-dependent DFT to reveal NIR transitions for the radical forms with n = 1 and 3 and a triplet ground state for the bis(*o*-semiquinone) dianion E^{2-}.

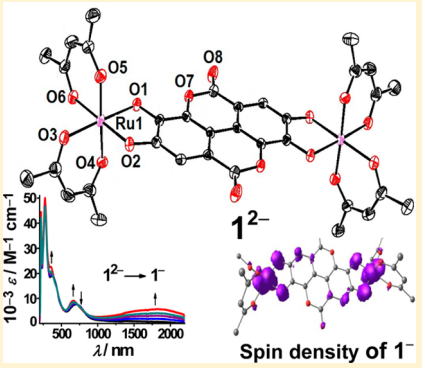

INTRODUCTION

The polyphenols constitute a major section of antioxidative natural products as found in various classes of organisms, including plants.[1] Their potential for (metalloenzyme-catalyzed) oxidation, for example, to quinones via radical intermediates may be considered as one possible mechanism of antioxidant activity. A particularly intriguing and widely distributed antioxidant occurring especially in nuts, berries, and other fruit as well as in wood (pulp processing, barrique treatment of wine) or other biomaterial is ellagic acid, EH_4, a symmetrical bis-catechol with a planar multicyclic conjugated π-system including two lactone rings.[2,3]

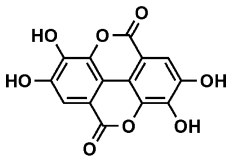

ellagic acid, EH_4

While the value of ellagic acid as a dietary supplement, for example, in the suppression of cancer[4] is not unambiguously proven, its potential as antioxidant is undisputed.[1,2] Although the interaction of metal ions with EH_4 or with its deprotonated ("ellagate") forms has long been known from the problem of wood processing,[3,5] from biomedical studies,[4,6] and from investigations concerning nanomaterials,[7] the binding of metals and their effect on the property and function of ellagic acid/ellagate have been reported only in a superficial way. In particular, a detailed investigation of the coordination chemistry in context with the redox behavior of the potentially noninnocent[8−10] ellagate polyphenolate has not yet been performed. Despite the apparent interest in the role of ellagic acid in various different sectors of applied chemistry,[1−7] rather little attention has been given to this remarkable molecule from mainstream chemistry.

The present study has thus been undertaken to deal with the question of suitability and potential of this naturally occurring oligophenol (bis-catechol) for metal binding and with the consequences for the redox behavior. Employing the unique chemistry[11] of ruthenium complexes with 1,2-dioxolene ligands, which provide the *o*-quinone/*o*-semiquinone/catecholate two-step redox system, our goal was to probe the metal stabilizing effect on various oxidation states and to identify the character of such states. Specific questions pertain to the potential formation of mixed-valent[11,12] dinuclear intermediates or of bridging ellagate or terminal radical ligands, the structural response to electron transfer, the stability of the ester functions, and the possible intramolecular interaction of the two metal-chelating dioxolene functions within a planar oligocyclic arrangement.

Considering our experience[13] with the fascinating interplay between 1,2-dioxolene redox-active ligands and the inert binding ruthenium ions (Ru^{II}, Ru^{III}, Ru^{IV}) as mimics of the lighter homologue iron, we set out to prepare and characterize

Received: August 15, 2015
Published: October 6, 2015

DOI: 10.1021/acs.inorgchem.5b01868
Inorg. Chem. 2015, 54, 10049−10057

dinuclear complexes of the potentially bis-chelating ligand E^{4-} and its neighboring oxidation states. The possible noninnocent behavior of E^{n-} was probed using structural, electrochemical, and spectroelectrochemical (UV−vis−NIR, electron paramagnetic resonance (EPR)) information. The experimental methodology is supported by DFT calculations, which are also used to assess the degree of metal−metal interaction, including possible mixed-valency,[11,12] in symmetrical dinuclear species $[L_2Ru(\mu\text{-}E)RuL_2]^n$, L = acetylacetonate ($acac^-$, 2,4-pentanedionate), 2,2′-bipyridine (bpy), or 2-phenylazopyridine (pap).

RESULTS AND DISCUSSION

Synthesis and Characterization. The dinuclear complexes $(NBu_4)_2[(acac)_2Ru^{III}(\mu\text{-}E^{4-})Ru^{III}(acac)_2]$ ($(NBu_4)_2$[**1**]), $[(bpy)_2Ru^{II}(\mu\text{-}E^{\bullet 3-})Ru^{II}(bpy)_2]ClO_4$ ([**2**]ClO_4), and $[(pap)_2Ru^{II}(\mu\text{-}E^{4-})Ru^{II}(pap)_2]$ ([**3**]) (Figure 1) were synthesized from the respective metal precursors *cis*-$Ru^{II}(acac)_2(CH_3CN)_2$, *cis*-$[Ru^{II}(bpy)_2(C_2H_5OH)_2]^{2+}$, or *cis-trans-cis*-$[Ru(pap)_2(C_2H_5OH)_2]^{2+}$ and ellagic acid (EH_4) in the presence of triethylamine as a base in refluxing ethanol. The complexes were isolated via chromatographic purification on a neutral alumina column. The presence of two chiral metal centers in the complexes leads to the possible formation of two diastereoisomeric forms, namely, *meso* (ΔΛ) and *rac* (ΔΔ/ΛΛ);[14] however, only one form has been selectively obtained in each case. The crystal structure of $(NBu_4)_2$[**1**] and the ^{1}H NMR spectra establish the *meso* form of $(NBu_4)_2$[**1**] and the *rac* forms of [**2**]ClO_4 or [**3**], respectively.

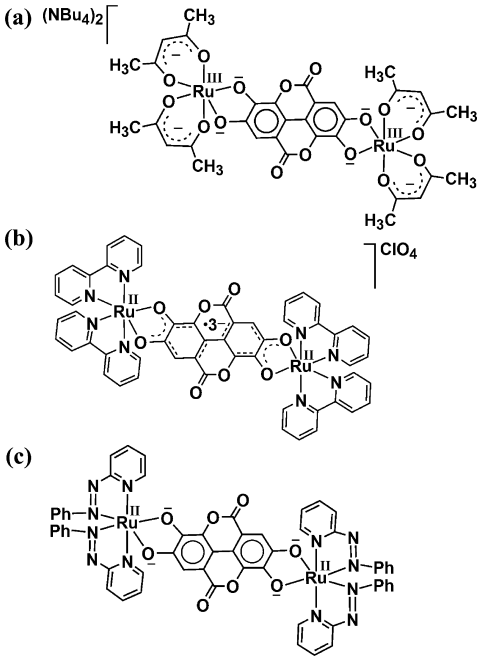

Figure 1. Representation of compounds (a) $(NBu_4)_2$[**1**], (b) [**2**]ClO_4, and (c) [**3**].

The complexes exhibit electrical conductivities and microanalytical and mass spectral properties in agreement with their formulation (see the Experimental Section and Figure S1). The meso diastereomeric form of $[\mathbf{1}]^{2-}$ with internal inversion center exhibits ^{1}H NMR resonances corresponding to the half of the molecule over a wide chemical shift range from 5 to −25 ppm in $(CD_3)_2SO$ (Figure S2) due to paramagnetic contact shift effects.[15] The complexes [**2**]ClO_4 and [**3**] in $(CD_3)_2SO$ display ^{1}H NMR signals corresponding to the full molecule in each case over chemical shift ranges from 15 to 6 ppm and from 9 to 6.5 ppm, respectively (Figure S2).

The chemical shifts in the ^{1}H NMR spectra indicate paramagnetism not only for the odd-electron species $\mathbf{2}^+$ but also for $\mathbf{1}^{2-}$, in agreement with a calculated triplet ground state and mixed spin distribution between the bridging ligand and both metal centers (see Tables below).

Crystal Structure of *meso*-$(NBu_4)_2$[1]. The bis(tetrabutylammonium) salt of $\mathbf{1}^{2-}$ crystallized with two independent molecules in the unit cell (Figure 2). The molecular parameters derived from structure analysis (Table 1 and Table S1) were not significantly different (Tables S2−S4 and Figure S3), Table 1 indicates a good reproduction for selected bond lengths by DFT.

In agreement with the connection of four nearly planar six-membered rings the bridging ligand on the whole is virtually planar (Figure 2b) and cannot twist such as the related systems $\mathbf{4}^{n+}$ and $\mathbf{5}^{n+}$ (Figure 3) in their fully oxidized (n = 4) or fully reduced forms (n = 0).[9,10]

The rigidity of the polycyclic system is also responsible for relatively small metrical effects as dependent on the oxidation state. Formally, the metal-coordinating OCCO chelates with their characteristic C−O bond lengths,[16] and the central C−C bond with its single/double bond character[9] (EH_4 vs EH_2, Figure 4) should indicate the oxidation state (Table 1, Tables S2−S8, and Figures S3−S5).

However, the size and rigidity of the polycyclic E^{n-} system allows only for small structural variations in the dinuclear compounds. The average C−O distance of 1.33 Å would be compatible with a catecholate/*o*-semiquinonate assignment as is the mean value of 1.42 Å for the central C−C bonds in $\mathbf{1}^{2-}$ (1.426 Å in EH_4[3]). The intramolecular metal−metal distances are rather long at ∼11.6 Å, while the shortest intermolecular Ru−Ru distance is only 7.6 Å. We therefore recur to spectroelectrochemical studies to extract the most appropriate oxidation state combinations of metals and terminal and bridging ligands.

Electrochemistry. The isolated complexes were studied by cyclic voltammetry (CV) and differential pulse voltammetry (DPV) in aprotic solution (Table 2, Figure 5, and Figure S6).

The bis-tetrabutylammonium salt of $\mathbf{1}^{2-}$ exhibits two reversible oxidation waves with a slight difference in intensity in the CV experiment; however, the DPV measurements confirm the equal amount of electrons being transferred (Figure S6). Further oxidation and reduction proceeds irreversibly under the chosen conditions, as observed also by spectroelectrochemistry (cf. below).

The compound [**2**]ClO_4 exhibits four reversible one-electron steps (Figure 5) in a similar fashion as the related system $\mathbf{4}^{n+}$.[9a] By comparison with $\mathbf{4}^{n+}$, the potentials (Table 2) are shifted by ∼0.3 V to higher values in $\mathbf{2}^{n+}$, caused by the acceptor effect from the lactone ester groups.

A further such anodic shift by ∼0.3 V is observed for system $\mathbf{3}^{n+}$, reflecting the stronger π-acceptor properties of the pap coligands relative to bpy. Additional four reductions in the form of two pairs of closely spaced waves take place for the pap coligands at negative potentials (<−1.0 V, Figure 5, Table 2). The potentials from Table 2 allowed us to calculate comproportionation constants K_c, especially for the paramagnetic intermediates. These values appear to illustrate the typical[9a] range of K_{c1} and K_{c3} from $1 \times 10^{4.0}$ to $1 \times 10^{6.5}$ for interaction between two molecular halves, whereas the larger

DOI: 10.1021/acs.inorgchem.5b01868
Inorg. Chem. 2015, 54, 10049−10057

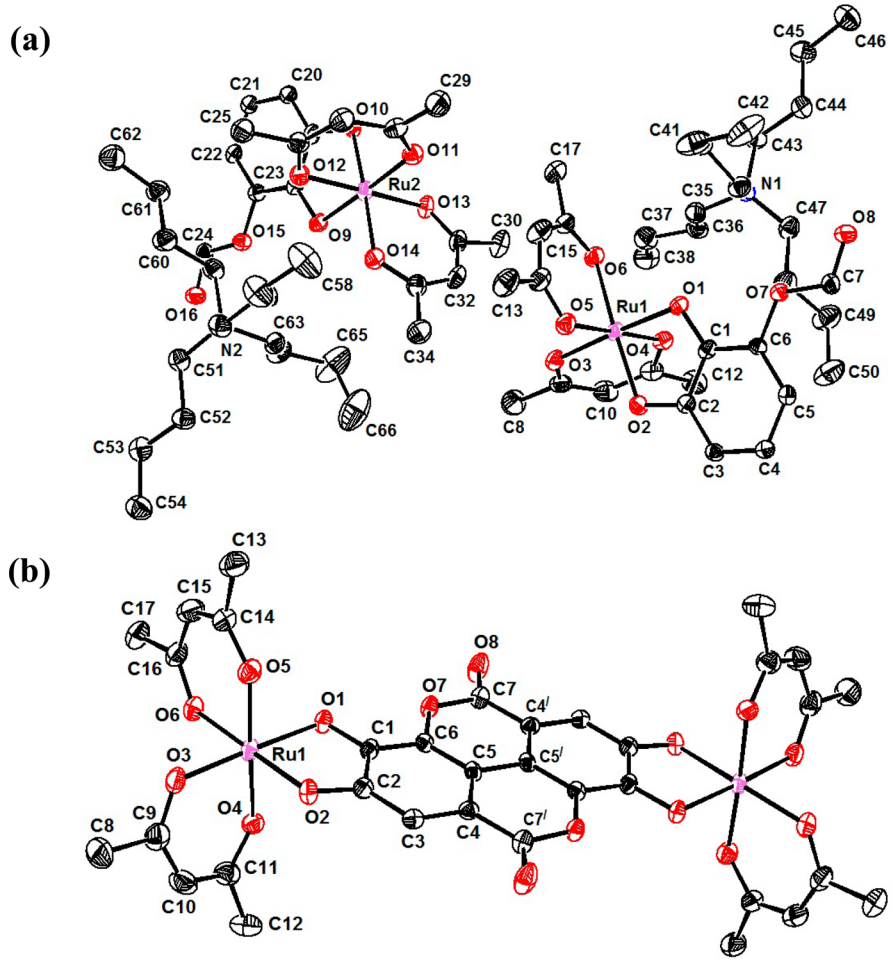

Figure 2. Molecular structure of *meso*-$(NBu_4)_2$[**1**] in the crystal; (a) asymmetric unit and (b) anionic part of one full molecule. Ellipsoids are drawn at 50% probability level. Hydrogen atoms are removed for clarity.

number of $K_{c2} = 1 \times 10^{10}$ to 1×10^{13} reflects the metal/chelate interaction. Similar effects were recorded earlier for system $\mathbf{4}^{n+}$.[9a] A rather large $K_{c4} = 1 \times 10^{8.1}$ is observed between the waves associated with reduction of same metal-coordinated pap coligands (cf. below).

Spectroelectrochemistry (UV−vis−NIR, EPR) and Time-Dependent DFT Calculations. Information from magnetic resonance (^{1}H NMR and EPR; Figures S2, S7, and S8) and UV−vis−NIR spectroelectrochemistry in conjunction with DFT-calculated spin densities (Figures 6−8, Table 3, and Figure S9) and time-dependent (TD) DFT calculated electronic transitions (Table 4, Tables S9−S11) serve to establish the most appropriate oxidation state combinations within the various charged forms of the dinuclear complexes (Scheme 1).

Starting with the structurally characterized $\mathbf{1}^{2-}$, this may be described by the two alternatives $Ru^{III}(\mu\text{-}E^{4-})Ru^{III}$ or $Ru^{II}(\mu\text{-}E^{\bullet 3-})Ru^{III}$. DFT calculations suggest a triplet ground state (Tables S12−S15) with spin density on the bridge and on both metals (Figure 6, Table 3), which is in agreement with the widely shifted ^{1}H NMR signals (Figure S2) and with a "hole mechanism" for donor bridge-mediated valence exchange.[12] No EPR signal could be detected down to 4 K. The lowest-energy transition at 712 nm is assigned to a ligand-to-metal charge transfer type of process (Table 4). The results point to comparable contributions from both the oxidation state descriptions given above.

The necessity to describe a $[Ru^n(Q^m)]^k$ charge form with more than one integer oxidation state combination n/m has been pointed out earlier based on experiment[11a] and theory.[11b] Remenyi and Kaupp have thus stated that "the true situation in a given complex may be intermediate between integer oxidation numbers".

Oxidation to $\mathbf{1}^-$ produces an EPR-silent[12] species even at 4 K and a near-IR absorption at 1785 nm (Figure 9). DFT calculations yield again spin densities on the metals and on the bridge where it is concentrated at the metal-coordinating chelate functions (Table 3, Figure 6, and Figure S9). The TD-DFT calculations point to an intraligand transition for the NIR band (Table 4). The formation of long-wavelength (NIR) absorptions in bridged dinuclear complexes with redox-active metals is frequently attributed to intervalence charge transfer or metal−metal charge transfer processes in mixed-valence situations.[12a,13] However, EPR studies and molecular orbital (MO) calculations (Tables S16−S31) may often correct such first-hand assignments because many radicals and radical complexes have also low-energy transitions involving the singly occupied MO.[17]

A TD-DFT calculation of the free ligand E^n, $n = 3-$, supports this intraligand transition assignment for $\mathbf{1}^-$, yielding a long-wavelength transition at 1487 nm (Table S11). The whole

DOI: 10.1021/acs.inorgchem.5b01868
Inorg. Chem. 2015, 54, 10049−10057

Table 1. Selected Experimental and DFT-Calculated Bond Lengths for *meso*-$(NBu_4)_2$[1][a]

	bond lengths (Å) of molecule I		bond lengths of molecule II	
	1^{2-} (X-ray)	1^{2-} (DFT)		1^{2-} (X-ray)
Ru1–O1	2.037(3)	2.052	Ru2–O9	2.046(3)
Ru1–O2	1.992(3)	2.014	Ru2–O10	1.993(3)
Ru1–O3	2.027(3)	2.096	Ru2–O11	2.025(3)
Ru1–O4	2.007(3)	2.067	Ru2–O12	2.009(3)
Ru1–O5	2.045(3)	2.072	Ru2–O13	2.040(3)
Ru1–O6	2.056(3)	2.095	Ru2–O14	2.029(3)
C1–O1	1.326(4)	1.305	C18–O9	1.323(4)
C2–O2	1.330(4)	1.323	C19–O10	1.339(4)
C7–O7	1.388(4)	1.386	C23–O15	1.402(4)
C6–O7	1.398(4)	1.381	C24–O15	1.382(4)
C7–O8	1.211(4)	1.219	C24–O16	1.213(5)
C1–C2	1.441(5)	1.446	C18–C19	1.437(5)
C1–C6	1.396(5)	1.415	C18–C23	1.391(5)
C2–C3	1.394(5)	1.403	C19–C20	1.392(5)
C3–C4	1.388(5)	1.398	C20–C21	1.387(5)
C4–C5	1.411(5)	1.420	C21–C22	1.416(5)
C4–C7′	1.462(5)	1.465	C21–C24′	1.464(5)
C5–C6	1.388(5)	1.393	C22–C23	1.387(5)
C5–C5′	1.433(7)	1.430	C22–C22′	1.414(7)

[a]Asymmetric unit of $(NBu_4)_2$[1] contains two independent molecules I and II.

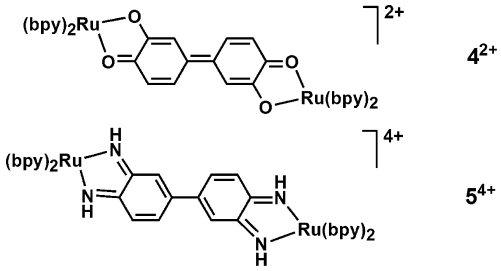

Figure 3. Representation of reported analogus ruthenium-bipyridine complexes.

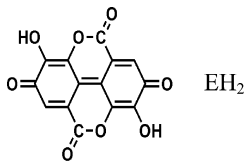

Figure 4. Representation of the doubly oxidized form of ellagic acid.

calculation series for E^{n-}, n = 1–4 (Tables S11 and S15), also suggests a triplet ground state for E^{2-} (Figure 10), involving the two connected but apparently weakly coupled coplanar *o*-semiquinones.

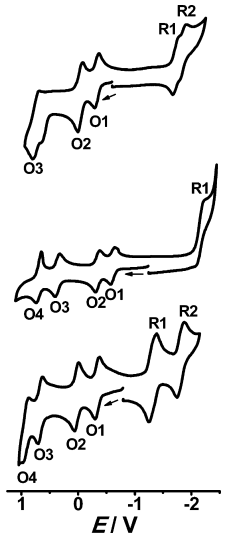

Figure 5. Cyclic voltammograms of *meso*-$(NBu_4)_2$[1] (upper), prereduced [2]ClO_4 (center) and [3] (lower) in Pt/CH_2Cl_2/0.1 M Bu_4NPF_6 vs Fc/Fc^+; scan rate 100 mV s^{-1}.

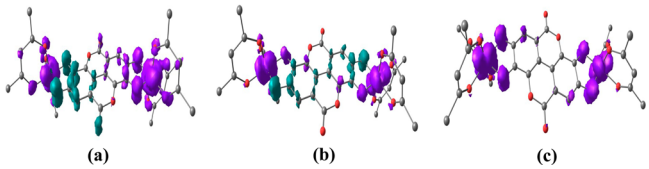

Figure 6. Spin-density representations of (a) **1** (S = 1), (b) $\mathbf{1}^-$ (S = 1/2), and (c) $\mathbf{1}^{2-}$ (S = 1).

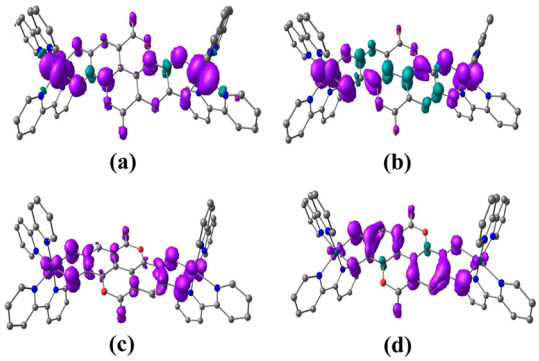

Figure 7. Spin-density representations of (a) $\mathbf{2}^{4+}$ (S = 1), (b) $\mathbf{2}^{3+}$ (S = 1/2), (c) $\mathbf{2}^{2+}$ (S = 1), and (d) $\mathbf{2}^{+}$ (S = 1/2).

It appears from these results that the $Ru^{III}(\mu\text{-}E^{\bullet 3-})Ru^{III}$ three-spin[18,14a] formulation is more appropriate for the oxidation state description of $\mathbf{1}^-$ than the alternative $Ru^{III}(\mu\text{-}E^{4-})Ru^{IV}$.

Table 2. Electrochemical Data[a]

	$E°_{298}$, V (ΔE, mV)[b]					
	ox4	ox3	ox2	ox1	red1	red2
$\mathbf{1}^{2-}$		0.80[c]	−0.04 (80)	−0.33 (80)	−1.76[c]	
$\mathbf{2}^{+}$	0.70 (90)	0.37 (60)	−0.35 (70)	−0.61 (80)	−2.20[c]	
3	0.92 (100)	0.67 (80)	0.03 (50)	−0.34 (60)	−1.32[d] (130)	−1.80[d] (130)

[a]From cyclic voltammetry in CH_2Cl_2/0.1 M Bu_4NPF6 at 100 mV s^{-1}. [b]Potential in volts vs Fc/Fc^+; peak potential differences ΔE, mV in parentheses. [c]Irreversible process. [d]Two-electron wave with small splitting (<80 mV).

DOI: 10.1021/acs.inorgchem.5b01868
Inorg. Chem. 2015, 54, 10049–10057

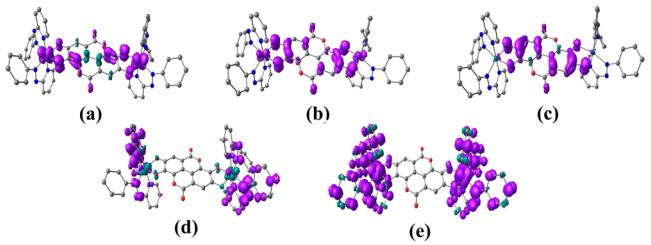

Figure 8. Spin-density representations of (a) 3^{3+} (S = 1/2), (b) 3^{2+} (S = 1), (c) 3^{+} (S = 1/2), (d) 3^{2-} (S = 1), and (e) 3^{4-} (S = 2).

Table 3. DFT-Calculated (UB3LYP/LanL2DZ/6-31G*) Mulliken Spin Densities

complex	Ru1	Ru2	E	acac$^-$
1 (S = 1)	0.704	0.957	0.009	0.330
1$^-$ (S = 1/2)	0.695	0.695	−0.506	0.116
1^{2-} (S = 1)	0.541	0.541	0.880	0.038
complex	Ru1	Ru2	E	bpy
2^{4+} (S = 1)	0.757	0.757	0.454	0.032
2^{3+} (S = 1/2)	0.343	0.343	0.318	−0.004
2^{2+} (S = 1)	0.187	0.187	1.646	−0.020
2^{+} (S = 1/2	0.033	0.033	0.946	−0.012
complex	Ru1	Ru2	E	pap
3^{3+} (S = 1/2)	0.230	0.230	0.556	−0.016
3^{2+} (S = 1)	0.113	0.113	1.790	−0.016
3^{+} (S = 1/2)	0.016	0.016	0.964	0.004
3^{2-} (S = 1)	−0.083	−0.083	−0.138	2.304
3^{4-} (S = 2)	0.559	0.559	0.250	2.632

The second oxidation to neutral **1** is accompanied by the formation of an NIR absorption at λ_{max} = 1080 nm, which is of mixed metal/ligand character (Figure 9, Table 4). The concentration of spin density on the metals and on acac$^-$ in

Scheme 1. Redox Transitions for Systems 1^n, 2^n, and 3^n with Assignments to Most Appropriate Oxidation States

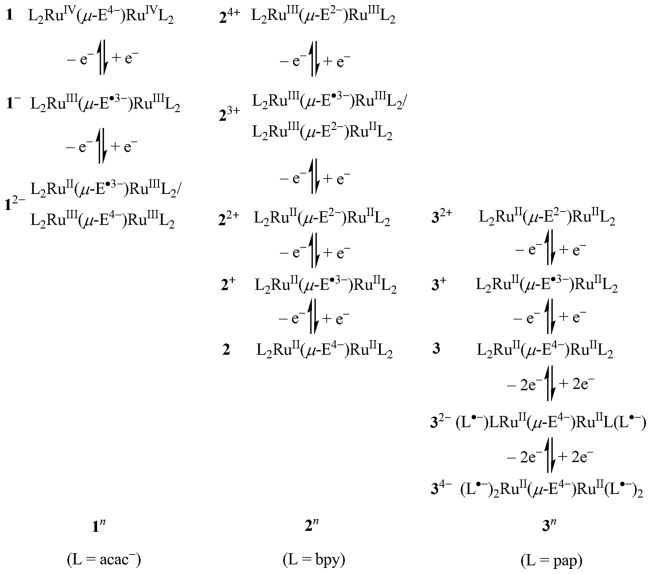

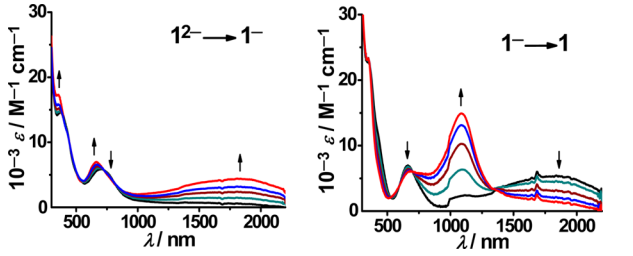

Figure 9. UV−vis−NIR spectroelectrochemistry of 1^n (n = 0,−,2−) in CH_2Cl_2/0.1 M Bu_4NPF_6.

Table 4. Experimental and TD-DFT ((U)B3LYP/CPCM/CH_2Cl_2) Calculated Electronic Transitions for 1^n

λ, nm (ε, M^{-1} cm^{-1}) (expt)	λ, nm (f) (DFT)[a]	transitions	character
1^{2-} (S = 1)			
712(5740)	879(0.46)	HOMO(β) → LUMO(β)(0.83)	E(π)/Ru(dπ) → Ru(dπ)/E(π*)
428sh	362(0.13)	HOMO(β) → LUMO+6(β)(0.29) HOMO−2(α) → LUMO(α)(0.29)	E(π)/Ru(dπ) → E(π*) Ru(dπ)/E(π) → acac(π*)
380(14 550)	352(0.16)	HOMO−2(α) → LUMO(α)(0.63)	Ru(dπ)/E(π) → acac(π*)
1$^-$ (S = 1/2)			
1785(4220)	1520(0.33)	SOMO → LUMO(α)(0.98)	E(π)/Ru(dπ) → E(π*)
665(6900)	811(0.17)	HOMO−4(α) → LUMO(α)(0.58)	Ru(dπ)/E(π) → E(π*)
	615(0.10)	HOMO−6(α) → LUMO(α)(0.55)	acac(π)/Ru(dπ) → E(π*)
		HOMO−1(β) → LUMO+1(β)(0.51)	Ru(dπ)/acac(π) → Ru(dπ)/E(π*)
	441(0.16)	HOMO(β) → LUMO+2(β)(0.86)	Ru(dπ)/E(π) → E(π*)
360(17 060)	348(0.11)	HOMO−2(β) → LUMO+2(β)(0.50) HOMO−11(β) → LUMO+1(β)(0.37)	E(π)/Ru(dπ) → E(π*) E(π) → Ru(dπ)/E(π*)
1 (S = 1)			
1087(14 790)	1142(0.07)	SOMO1 → LUMO(α)(0.83)	E(π)/Ru(dπ) → E(π*)/Ru(dπ)
	1065(0.14)	HOMO(β) → LUMO(β)(0.71)	E(π)/Ru(dπ) → E(π*)/Ru(dπ)
	921(0.07)	HOMO−4(α) → LUMO(α)(0.47) SOMO1 → LUMO(α)(0.40)	acac(π)/Ru(dπ) → E(π*)/Ru(dπ) E(π)/Ru(dπ) → E(π*)/Ru(dπ)
660(5940)	681(0.04)	HOMO(β) → LUMO+2(β)(0.48) HOMO−1(β) → LUMO+2(β)(0.35)	E(π)/Ru(dπ) → Ru(π) Ru(dπ)/acac(π)/E(π) → Ru(π)
350sh	322(0.07)	HOMO−2(β) → LUMO+4(β)(0.53) HOMO−11(β) → LUMO+1(β)(0.32)	Ru(dπ)/acac(π) → acac(π*) acac(π)/Ru(dπ) → Ru(dπ)/E(π*)

[a]Transitions with f > 0.04.

DOI: 10.1021/acs.inorgchem.5b01868
Inorg. Chem. 2015, 54, 10049−10057

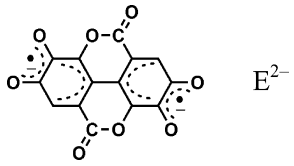

Figure 10. Representation of the doubly oxidized form of deprotonated ellagic acid (E^{2-}).

the triplet ground state suggests an oxidation to Ru^{IV} instead of E^{2-} (Table 3).

The $\mathbf{2}^{+}$ ion in the isolated compound $[\mathbf{2}]ClO_4$ is best formulated as a $Ru^{II}(\mu\text{-}E^{\bullet 3-})Ru^{II}$ species (Figure S4 and Tables S13 and S15). The EPR at $g \approx 2.03$, the spin density concentrated on the bridge (Figure 7, Table 3), and the long-wavelength (NIR) absorptions with intraligand (IL, at 2135 nm) and metal-to-ligand charge transfers (MLCT) character (at 1100 nm) are all confirming this assignment. Reduction leads to the singlet species **2** with $Ru^{II}(\mu\text{-}E^{4-})Ru^{II}$ configuration and weak $\pi(E^{4-}) \rightarrow \pi^*$(bpy) ligand-to-ligand charge transfer (LLCT) and typical metal-to-ligand charge transfers (MLCT) $d\pi(Ru) \rightarrow \pi^*$(bpy) transitions (Table S9).

Oxidation of $\mathbf{2}^{+}$ is assumed to occur at the bridge, with little changed EPR resonance and low-energy transitions (MLCT, IL, Figure 11) involving the π^* orbital of partially oxidized E^{n-}

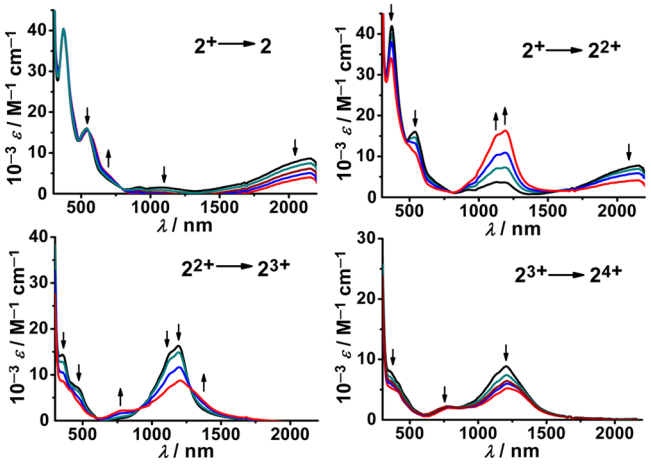

Figure 11. UV−vis−NIR spectroelectrochemistry of $\mathbf{2}^{n}$ (n = 4+,3+,2+, +, 0) in CH_2Cl_2/0.1 M Bu_4NPF_6.

(n = 2). The next oxidation to $\mathbf{2}^{3+}$ is formulated as leading to a mixed system involving $Ru^{III}(\mu\text{-}E^{\bullet 3-})Ru^{III}$ and $Ru^{II}(\mu\text{-}E^{2-})Ru^{III}$ contributions, retaining the band system at ∼1200 nm in diminished form. Oxidation to $\mathbf{2}^{4+}$ is assigned to produce a $Ru^{III}(\mu\text{-}E^{2-})Ru^{III}$ formulation with a still further diminished 1200 nm absorption, again attributed to transitions between largely Ru/E-mixed frontier orbitals. These features are similarly observed for system $\mathbf{4}^{n+}$.[9a]

Using the pap coligand, which is a strong π-acceptor and tends to stabilize exclusively ruthenium(II), the isolated nonmagnetic (NMR, EPR) neutral form **3** is formulated as $Ru^{II}(\mu\text{-}E^{4-})Ru^{II}$ (Figure S5, Tables S14 and S15), which can be ligand-oxidized to $Ru^{II}(\mu\text{-}E^{\bullet 3-})Ru^{II}$ with bridge-based spin. The EPR signal for $\mathbf{3}^{+}$ at 120 K (g_1 = 2.011, g_2 = 2.002, g_3 = 1.987) and the DFT-calculated spin densities (Table 3, Figure 8, and Figure S7) confirm this assignment, as does the intense absorption around 2000 nm, assigned to a donor ligand ($E^{\bullet 3-}$) to π-acceptor ligand (pap) transition (ligand-to-ligand charge transfer; see Figure 12). Actually, most electronic transitions in the $\mathbf{3}^{n}$ series have the π^*(pap) orbitals as target (Tables S10 and S11). Reversible reduction is also possible, taking place at the pap ancillary ligands according to calculated spin densities (Table 3 and Figure 8) and experimental EPR results with slightly diminished[19] g values ($\mathbf{3}^{2-}$), 120 K: g_1 = 2.021, g_2 = 1.990, g_3 = 1.973, Figure S8).

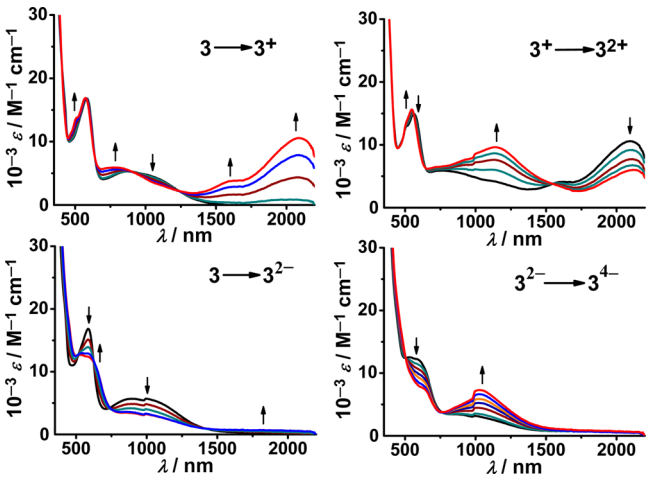

Figure 12. UV−vis−NIR spectroelectrochemistry of $\mathbf{3}^{n}$ in CH_2Cl_2/0.1 M NBu_4PF_6.

CONCLUSION

In addition to its numerous and diverse biological and physiological functions[2−7] the ellagic acid/ellagate system represents a remarkable ligand for coordination chemistry. Our present study of diruthenium complexes shows that ellagate is a symmetrically dinucleating bis-chelate ligand, involving two conjugated and lactone acceptor-connected redox-active catecholate functions within an essentially planar polycyclic arrangement. There is clearly potential for non-innocent ligand behavior with several conceivable charge states of E^{n-}, n = 1−4.

Our investigations of three redox systems with donating ($acac^-$) or differently accepting (bpy, pap) coligands at ruthenium suggest that the well-established[11] strong coupling between *o*-semiquinone chelates and Ru^{II} or Ru^{III} leads to relatively weak interactions *within* the bridging ligand. The connection of the dioxolene moieties by one CC bond and two ester functions in the lactone rings is more relevant for the thus-enforced planarity than for electronic coupling. No evidence has been found for any reactivity of the lactone functions under the aprotic conditions employed. As a consequence of the rigid polycyclic configuration, the structural changes for the various states $\mu\text{-}E^{n-}$ of the bridge were calculated to be rather small in the complexes, affecting the use of experimental structure data for oxidation state assignment. Radical intermediates were identified by EPR, whereas mixed-valent formulations play a minor role. The results obtained here confirm the similarity of systems $\mathbf{2}^{n+}$ and $\mathbf{4}^{n+}$ except for the "decoupled" doubly reduced (n = 0) and doubly oxidized forms (n = 4), as presumed by Ward and co-workers who invoked twisting around the central CC bond.[9a]

While the suitability of conformationally rigid ellagate in various charge states E^{n-} as a noninnocently behaving bis-bidentate bridging ligand is demonstrated in the present article

DOI: 10.1021/acs.inorgchem.5b01868
Inorg. Chem. 2015, 54, 10049−10057

using prototypical ruthenium complex fragments, the observed radical complex formation and the potential for metal−metal valence exchange may also be investigated for other transition metal compounds of this antioxidative polyphenol π-system. The TD-DFT calculations presented here for uncoordinated E^{n-} constitute a basis for possible uses of this ligand in coordination chemistry. Thus, the presence of two coplanar but weakly coupled catecholate/*o*-semiquinonate chelate sites may invite studies of magnetism,[20] and the bis-bidentate chelate function can become part of redox-active coordination polymer frameworks.[21]

EXPERIMENTAL SECTION

Materials. The precursor complexes *cis*-Ru(acac)$_2$(CH$_3$CN)$_2$,[22] *cis*-Ru(bpy)$_2$Cl$_2$,[23] and *cis-trans-cis*-Ru(pap)$_2$Cl$_2$[24] were prepared according to procedures reported in literature. The ligand ellagic acid (EH_4) was purchased from Alfa Aesar. Other chemicals and solvents were of reagent grade and used as received. For spectroscopic and electrochemical studies HPLC grade solvents were used.

Physical Measurements. The electrical conductivity of the solution was checked by using an autoranging conductivity meter (Toshcon Industries, India). The EPR measurements were made in a two-electrode capillary tube[19] with an X-band (9.5 GHz) Bruker system ESP300 spectrometer. Cyclic voltammetric and differential pulse voltammetric measurements of the complexes in the isolated native state were done using a PAR model 273A electrochemistry system. Glassy carbon working electrode, platinum wire auxiliary electrode, and saturated calomel reference electrode (SCE) were used in a standard three-electrode configuration with tetraethylammonium perchlorate as the supporting electrolyte (substrate concentration ≈ 1×10^{-3} M; standard scan rate 100 mV s^{-1}; ***Caution!*** *Perchlorate salts are explosive and should be handled with care*). UV−vis−NIR spectroelectrochemical studies were performed in CH$_2$Cl$_2$/0.1 M Bu_4NPF_6 at 298 K using an optically transparent thin-layer electrode cell[25] mounted in the sample compartment of a J&M TIDAS spectrophotometer. All spectroelectrochemical experiments were performed under a dinitrogen atmosphere. ^{1}H NMR spectra were recorded on a Bruker Avance III 400 MHz spectrometer. The elemental analyses were recorded on a PerkinElmer 240C elemental analyzer. Fourier-transform IR spectra were recorded on a Nicolet spectrophotometer; the samples were prepared as KBr pellets. Electrospray mass spectral measurements were done on a Micromass Q-ToF mass spectrometer.

Preparation of Complexes. *Synthesis of $(NBu_4)_2[Ru_2(acac)_4(\mu\text{-}E)]$, $(NBu_4)_2$[**1**].* A mixture comprising *cis*-Ru(acac)$_2$(CH$_3$CN)$_2$ (100 mg, 0.26 mmol), the ligand EH_4 (40 mg, 0.13 mmol), and NEt_3 (0.08 mL, 0.54 mmol) in 50 mL of EtOH was heated to reflux for 8 h under a dinitrogen atmosphere. The solvent was then removed, and the residue was moistened with a few drops of CH$_3$CN. The addition of a saturated aqueous solution of NBu_4Br led to the precipitation of the desired complex, which was filtered, washed with chilled water to remove excess NBu_4Br, and dried in vacuo over P_4O_{10}. The product was purified further on a neutral alumina column, and the green complex $(NBu_4)_2$[**1**] was eluted by a 30:1 CH$_2$Cl$_2$/CH$_3$OH mixture. The solvent was removed to yield pure $(NBu_4)_2$[**1**]. Yield: 142 mg (78%). MS (ESI+, CH$_3$OH): *m*/*z* {$(NBu_4)_2$[**1**]}$^+$ calcd: 1382.53; found: 1382.48. ^{1}H NMR (400 MHz) in (CD$_3$)$_2$SO [δ, ppm (*J*, Hz)]: 4.4 (s, 2H(E)), 4.23 (s, 6H(CH$_3$-acac)), 3.18 (m, 16H), 2.99 (s, 6H(CH$_3$-acac)), 1.55 (m, 16H), 1.31 (m, 16H), 0.95 (t, 7, 24H), −3.01 (s, 6H(CH$_3$-acac)), −10.95 (s, 6H(CH$_3$-acac)), −20.3 (s, 2H(CH-acac)), −24.7 (s, 2H(CH-acac)). IR (KBr): ν(CO, cm^{-1}): 1698, 1678. Anal. Calcd (%) for $C_{66}H_{102}N_2O_{16}Ru_2$: C, 57.37; H, 7.44; N, 2.03; found: C, 57.10; H, 7.40; N, 2.14. Molar conductivity (CH$_2$Cl$_2$): Λ_M = 185 Ω^{-1} cm^2 M^{-1}.

*Synthesis of $[Ru_2(bpy)_4(\mu\text{-}E)]ClO_4$, [**2**]$ClO_4$.* The starting complex *cis*-Ru(bpy)$_2$(Cl)$_2$ (100 mg, 0.21 mmol) and $AgClO_4$ (87.07 mg, 0.42 mmol) were taken in 50 mL of EtOH and refluxed for 2 h. The precipitated AgCl was filtered off through a sintered Gooch crucible. The filtrate, the ligand EH_4 (32 mg, 0.105 mmol), and NEt_3 (0.06 mL, 0.42 mmol) were heated to reflux for 12 h under a dinitrogen atmosphere. The solvent was evaporated, and the residue was moistened with a few drops of CH$_3$OH, followed by the addition of a saturated aqueous $NaClO_4$ solution. The precipitate thus obtained was filtered, washed with chilled water to remove excess $NaClO_4$, and then dried in vacuo over P_4O_{10}. The product was purified on a neutral alumina column, and the brown complex [**2**]ClO_4 was eluted by 15:1 CH$_2$Cl$_2$/CH$_3$OH mixture. The solvent was removed to yield pure [**2**]ClO_4. Yield: 85 mg (67%). MS (ESI+, CH$_3$OH): *m*/*z* {[**2**]}$^+$: calcd: 1126.07; found: 1126.06. ^{1}H NMR (400 MHz) in (CD$_3$)$_2$SO [δ, ppm (*J*, Hz)]: 14.4 (m, 3H), 12.4 (m, 3H), 10.55 (m, 3H), 9.4 (m, 2H), 8.3 (m, 13H), 7.35 (m, 3H), 6.85 (m, 3H), 6.75 (m, 1H), 6.05 (m, 3H). IR (KBr): ν(CO, cm^{-1}): 1690, 1666, ν(ClO_4^-, cm^{-1}): 1085, 621. Anal. Calcd (%) for $C_{54}H_{34}ClN_8O_{12}Ru_2$: C, 52.97; H, 2.80; N, 9.15; found: C, 52.66; H, 2.98; N, 9.25. Molar conductivity (CH$_2$Cl$_2$): Λ_M = 94 Ω^{-1} cm^2 M^{-1}.

*Synthesis of $[Ru_2(pap)_4(\mu\text{-}E)]$, [**3**].* The starting complex *cis-trans-cis*-Ru(pap)$_2$Cl$_2$ (100 mg, 0.19 mmol) and $AgClO_4$ (79.04 mg, 0.38 mmol) were taken in EtOH and refluxed for 2 h. The precipitated AgCl was removed by filtering the mixture through a sintered Gooch crucible. The filtrate was mixed with the ligand EH_4 (28 mg, 0.095 mmol) and NEt_3 (0.06 mL, 0.42 mmol) and heated to reflux for 10 h under a dinitrogen atmosphere. The solvent was evaporated under reduced pressure, and the residue was extracted by dichloromethane. The solid product thus obtained on removal of solvent under reduced pressure was washed several times with ice-cold water and dried under vacuum over P_4O_{10}. It was then purified on a neutral alumina column using CH$_2$Cl$_2$/CH$_3$OH (40:1) mixture as eluent. The solvent was evaporated under reduced pressure to yield the pure complex [**3**]. Yield: 70 mg (60%). ESI MS(+) (in CH$_3$OH): *m*/*z* calcd for {[**3**]}$^+$: 1234.10; found: 1234.07. ^{1}H NMR (400 MHz, (CD$_3$)$_2$SO, 298 K, TMS): δ, ppm = 8.78 (m, 4H), 8.39 (m, 1H), 8.25 (m, 3H), 8.1 (m, 2H), 7.85 (m, 4H), 7.7 (m, 2H), 7.4 (m, 4H), 7.2 (m, 9H), 7.05 (m, 2H), 6.8 (m, 4H), 6.65 (m, 3H); IR (KBr): ν(CO, cm^{-1}): 1686, 1669; Anal. Calcd (%) for $C_{58}H_{38}N_{12}O_8Ru_2$: C, 56.49; H, 3.11; N, 13.63; found: C, 56.75; H, 3.30; N, 13.25. Molar conductivity (CH$_2$Cl$_2$): Λ_M = 9 Ω^{-1} cm^2 M^{-1}.

Crystal Structure Determination. Single crystals of $(NBu_4)_2$[**1**] were grown by slow evaporation of a 1:1 CH$_2$Cl$_2$/CH$_3$OH solution. X-ray diffraction data were collected using a Rigaku Saturn-724+ CCD single-crystal diffractometer using Mo Kα radiation. The data collection was evaluated by using the CrystalClear-SM Expert software. The data were collected by the standard ω-scan technique. The structure was solved by direct method using SHELXS-97 and refined by full matrix least-squares with SHELXL-97, refining on F^2.[26] All data were corrected for Lorentz and polarization effects, and all non-hydrogen atoms were refined anisotropically. The remaining hydrogen atoms were placed in geometrically constrained positions and refined with isotropic temperature factors, generally 1.2U_{eq} of their parent atoms. Hydrogen atoms were included in the refinement process as per the riding model. Additional crystallographic information is available in the Supporting Information.

Computational Details. Full geometry optimizations were performed using the DFT method at the (U)B3LYP level for $\mathbf{1}^n$ (n = +, 0, −, 2−, 3−), $\mathbf{2}^n$ (n = 4+, 3+, 2+, +), $\mathbf{3}^n$ (n = 3+, 2+, +, 2−, 4−), and (R)B3LYP for **2** and **3**.[27] All elements except ruthenium were assigned the 6-31G(d) basis set. The LanL2DZ basis set with effective core potential was employed for the ruthenium atom.[28] All calculations were performed with the Gaussian09 program package.[29] Vertical electronic excitations based on (U)B3LYP optimized geometries were computed using the TD-DFT formalism[30] in dichloromethane using the conductor-like polarizable continuum model (CPCM).[31] Chemissian 1.7[32] was used to calculate the fractional contributions of various groups to each molecular orbital. All the calculated structures were visualized with ChemCraft.[33]

DOI: 10.1021/acs.inorgchem.5b01868
Inorg. Chem. 2015, 54, 10049−10057

■ ASSOCIATED CONTENT

Supporting Information

The Supporting Information is available free of charge on the ACS Publications website at DOI: 10.1021/acs.inorgchem.5b01868. CCDC-1410538 ($(NBu_4)_2$[**1**]) contains the supplementary crystallographic data for this paper. These data can be obtained free of charge from The Cambridge Crystallographic Data Centre via www.ccdc.cam.ac.uk/data_request/cif.

X-ray data for compound $(NBu_4)_2$[**1**]. (CIF)
Figures: Mass spectra, ^{1}H NMR, DFT optimized structures, CV and DPV, EPR, spin density. Tables: crystal data, bond lengths and angles (DFT), TD-DFT, energy, MO compositions. (PDF)

■ AUTHOR INFORMATION

Corresponding Authors

*E-mail: lahiri@chem.iitb.ac.in. (G.K.L.)
*E-mail: kaim@iac.uni-stuttgart.de. (W.K.)

Notes

The authors declare no competing financial interest.

■ ACKNOWLEDGMENTS

Financial support received from the Department of Science and Technology, Council of Scientific and Industrial Research (fellowship to A.M.), New Delhi (India), the Land Baden-Württemberg (Germany) is gratefully acknowledged.

■ REFERENCES

(1) Quideau, S.; Deffieux, D.; Douat-Casassus, C.; Pouységu, L. *Angew. Chem.* **2011**, *123*, 610−646; *Angew. Chem., Int. Ed.* **2011**, *50*, 586−621.

(2) *Chemistry and Biology of Ellagitannins;* Quideau, S., Ed.; World Scientific Publishing: Singapore, 2009.

(3) McL Mathieson, A.; Poppleton, B. J. *Acta Crystallogr., Sect. B: Struct. Crystallogr. Cryst. Chem.* **1968**, *B24*, 1456−1461.

(4) (a) Takagi, A.; Sai, K.; Umemura, T.; Hasegawa, R.; Kurokawa, Y. *Cancer Lett.* **1995**, *95*, 139−144. (b) Fjaeraa, C.; Nånberg, E. *Biomed. Pharmacother.* **2009**, *63*, 254−261.

(5) Hewitt, D. G.; Nelson, P. F. *Holzforschung* **1965**, *19*, 97.

(6) (a) Bock, P. E.; Srinivasan, K. R.; Shore, J. D. *Biochemistry* **1981**, *20*, 7258−7266. (b) Ahmed, S.; Rahman, A.; Saleem, M.; Athar, M.; Sultana, S. *Hum. Exp. Toxicol.* **1999**, *18*, 691−698. (c) Marković, Z.; Milenković, D.; Đorović, J.; Dimitrić Marković, J. M. D.; Lučić, B.; Amić, D. *Monatsh. Chem.* **2013**, *144*, 803−812. (d) Huang, S.-T.; Yang, R. C.; Wu, H.-T.; Wang, C.-N.; Pang, J.-H. S. *PLoS One* **2011**, *6*, e18986.

(7) (a) Barnaby, S. N.; Yu, S. M.; Fath, K. R.; Tsiola, A.; Khalpari, O.; Banerjee, I. A. *Nanotechnology* **2011**, *22*, 225605. (b) Behl, G.; Sharma, M.; Dahiya, S.; Chhikara, A.; Chopra, M. *J. Nanomater.* **2011**, *2011*, 1, DOI: 10.1155/2011/695138. (c) Yuvakkumar, R.; Nathanael, A. J.; Hong, S. I. *RSC Adv.* **2014**, *4*, 44495−44499.

(8) (a) Kaim, W.; Schwederski, B. *Coord. Chem. Rev.* **2010**, *254*, 1580−1588. (b) Kaim, W. *Inorg. Chem.* **2011**, *50*, 9752−9765. (c) Kaim, W. *Eur. J. Inorg. Chem.* **2012**, *2012*, 343−348.

(9) (a) Joulié, L. F.; Schatz, E.; Ward, M. D.; Weber, F.; Yellowlees, L. H. *J. Chem. Soc., Dalton Trans.* **1994**, 799−804. (b) Auburn, P. R.; Lever, A. B. P. *Inorg. Chem.* **1990**, *29*, 2551−2553.

(10) (a) Patra, S.; Sarkar, B.; Ghumaan, S.; Fiedler, J.; Zalis, S.; Kaim, W.; Lahiri, G. K. *Dalton Trans.* **2004**, 750−753.

(11) (a) Kaim, W.; Lahiri, G. K. *Angew. Chem.* **2007**, *119*, 1808−1828; *Angew. Chem., Int. Ed.* **2007**, *46*, 1778−1796. (b) Ernst, S.; Hänel, P.; Jordanov, J.; Kaim, W.; Kasack, V.; Roth, E. *J. Am. Chem. Soc.* **1989**, *111*, 1733−1738. (c) Kasack, V.; Kaim, W.; Binder, H.; Jordanov, J.; Roth, E. *Inorg. Chem.* **1995**, *34*, 1924−1933.

(12) (a) Creutz, C. *Prog. Inorg. Chem.* **1983**, *30*, 1. (b) Rocha, R. C.; Rein, F. N.; Jude, H.; Shreve, A. P.; Concepcion, J. J.; Meyer, T. J. *Angew. Chem.* **2008**, *120*, 513−516; *Angew. Chem., Int. Ed.* **2008**, *47*, 503−506. (c) Agarwala, H.; Scherer, T.; Maji, S.; Mondal, T. K.; Mobin, S. M.; Fiedler, J.; Urbanos, F. A.; Jiménez-Aparicio, R.; Kaim, W.; Lahiri, G. K. *Chem.—Eur. J.* **2012**, *18*, 5667−5675.

(13) (a) Patra, S.; Sarkar, B.; Mobin, S. M.; Kaim, W.; Lahiri, G. K. *Inorg. Chem.* **2003**, *42*, 6469−6473. (b) Remenyi, C.; Kaupp, M. *J. Am. Chem. Soc.* **2005**, *127*, 11399−11413.

(14) (a) Kumbhakar, D.; Sarkar, B.; Maji, S.; Mobin, S. M.; Fiedler, J.; Urbanos, F. A.; Jiménez-Aparicio, R.; Kaim, W.; Lahiri, G. K. *J. Am. Chem. Soc.* **2008**, *130*, 17575−11583. (b) Mandal, A.; Agarwala, H.; Ray, R.; Plebst, S.; Mobin, S. M.; Priego, J. L.; Jiménez-Aparicio, R.; Kaim, W.; Lahiri, G. K. *Inorg. Chem.* **2014**, *53*, 6082−6093. (c) Sarkar, B.; Patra, S.; Fiedler, J.; Sunoj, R. B.; Janardanan, D.; Mobin, S. M.; Niemeyer, M.; Lahiri, G. K.; Kaim, W. *Angew. Chem.* **2005**, *117*, 5800−5803; *Angew. Chem., Int. Ed.* **2005**, *44*, 5655−5658. (d) Sarkar, B.; Patra, S.; Fiedler, J.; Sunoj, R. B.; Janardanan, D.; Lahiri, G. K.; Kaim, W. *J. Am. Chem. Soc.* **2008**, *130*, 3532−3542.

(15) (a) Das, A.; Scherer, T.; Maji, S.; Mondal, T. K.; Mobin, S. M.; Urbanos, F. A.; Jiménez-Aparicio, R.; Kaim, W.; Lahiri, G. K. *Inorg. Chem.* **2011**, *50*, 7040−7049. (b) Maji, S.; Sarkar, B.; Mobin, S. M.; Fiedler, J.; Urbanos, F. A.; Jimenez-Aparicio, R.; Kaim, W.; Lahiri, G. K. *Inorg. Chem.* **2008**, *47*, 5204−5211. (c) Koiwa, T.; Masuda, Y.; Shono, J.; Kawamoto, Y.; Hoshino, Y.; Hashimoto, T.; Natarajan, K.; Shimizu, K. *Inorg. Chem.* **2004**, *43*, 6215−6223. (d) Eaton, D. R. *J. Am. Chem. Soc.* **1965**, *87*, 3097−3102. (e) Holm, R. H.; Cotton, F. A. *J. Am. Chem. Soc.* **1958**, *80*, 5658−5663.

(16) Bhattacharya, S.; Gupta, P.; Basuli, F.; Pierpont, C. G. *Inorg. Chem.* **2002**, *41*, 5810−5816.

(17) Kaim, W. *Coord. Chem. Rev.* **2011**, *255*, 2503−2513.

(18) (a) Ye, S.; Sarkar, B.; Lissner, F.; Schleid, T.; van Slageren, J.; Fiedler, J.; Kaim, W. *Angew. Chem.* **2005**, *117*, 2140−2143; *Angew. Chem., Int. Ed.* **2005**, *44*, 2103−2106. (b) Paretzki, A.; Hübner, R.; Ye, S.; Bubrin, M.; Kämper, S.; Kaim, W. *J. Mater. Chem. C* **2015**, *3*, 4801−4809.

(19) Kaim, W.; Ernst, S.; Kasack, V. *J. Am. Chem. Soc.* **1990**, *112*, 173−178.

(20) Woods, T. J.; Ballesteros-Rivas, M. F.; Ostrovsky, S. M.; Palii, A. V.; Reu, O. S.; Klokishner, S. I.; Dunbar, K. R. *Chem. - Eur. J.* **2015**, *21*, 10302−10305.

(21) (a) Leong, C. F.; Chan, B.; Faust, T. B.; Turner, P.; D'Alessandro, M. D. *Inorg. Chem.* **2013**, *52*, 14246−14252. (b) Faust, T. B.; D'Alessandro, D. M. *RSC Adv.* **2014**, *4*, 17498−17512.

(22) Kobayashi, T.; Nishina, Y.; Shimizu, K. G.; Satô, G. P. *Chem. Lett.* **1988**, 1137−1140.

(23) Sullivan, B. P.; Salmon, D. J.; Meyer, T. J. *Inorg. Chem.* **1978**, *17*, 3334−3341.

(24) Goswami, S.; Chakravarty, A. R.; Chakravorty, A. *Inorg. Chem.* **1983**, *22*, 602−609.

(25) Krejcik, M.; Danek, M.; Hartl, F. *J. Electroanal. Chem. Interfacial Electrochem.* **1991**, *317*, 179−187.

(26) (a) Sheldrick, G. M. *Acta Crystallogr., Sect. A: Found. Crystallogr.* **2008**, *A64*, 112−122. (b) *Program for Crystal Structure Solution and Refinement;* University of Göttingen: Göttingen, Germany, 1997.

(27) Lee, C.; Yang, W.; Parr, R. G. *Phys. Rev. B: Condens. Matter Mater. Phys.* **1988**, *37*, 785−789.

(28) (a) Andrae, D.; Haeussermann, U.; Dolg, M.; Stoll, H.; Preuss, H. *Theor. Chim. Acta* **1990**, *77*, 123−141. (b) Fuentealba, P.; Preuss, H.; Stoll, H.; von Szentpaly, L. *Chem. Phys. Lett.* **1982**, *89*, 418−422.

(29) Frisch, M. J.; Trucks, G. W.; Schlegel, H. B.; Scuseria, G. E.; Robb, M. A.; Cheeseman, J. R.; Scalmani, G.; Barone, V.; Mennucci, B.; Petersson, G. A.; Nakatsuji, H.; Caricato, M.; Li, X.; Hratchian, H. P.; Izmaylov, A. F.; Bloino, J.; Zheng, G.; Sonnenberg, J. L.; Hada, M.; Ehara, M.; Toyota, K.; Fukuda, R.; Hasegawa, J.; Ishida, M.; Nakajima, T.; Honda, Y.; Kitao, O.; Nakai, H.; Vreven, T.; Montgomery Jr., J. A.; Peralta, J. E.; Ogliaro, F.; Bearpark, M.; Heyd, J. J.; Brothers, E.; Kudin, K. N.; Staroverov, V. N.; Kobayashi, R.; Normand, J.; Raghavachari, K.;

DOI: 10.1021/acs.inorgchem.5b01868
Inorg. Chem. 2015, 54, 10049−10057

Rendell, A.; Burant, J. C.; Iyengar, S. S.; Tomasi, J.; Cossi, M.; Rega, N.; Millam, J. M.; Klene, M.; Knox, J. E.; Cross, J. B.; Bakken, V.; Adamo, C.; Jaramillo, J.; Gomperts, R.; Stratmann, R. E.; Yazyev, O.; Austin, A. J.; Cammi, R.; Pomelli, C.; Ochterski, J. W.; Martin, R. L.; Morokuma, K.; Zakrzewski, V. G.; Voth, G. A.; Salvador, P.; Dannenberg, J. J.; Dapprich, S.; Daniels, A. D.; Farkas, O.; Foresman, J. B.; Ortiz, J. V.; Cioslowski, J.; Fox, D. J. *Gaussian 09,* Revision A.02; Gaussian, Inc: Wallingford, CT, 2009.

(30) (a) Bauernschmitt, R.; Ahlrichs, R. *Chem. Phys. Lett.* **1996**, *256*, 454−464. (b) Stratmann, R. E.; Scuseria, G. E.; Frisch, M. J. *J. Chem. Phys.* **1998**, *109*, 8218−8225. (c) Casida, M. E.; Jamorski, C.; Casida, K. C.; Salahub, D. R. *J. Chem. Phys.* **1998**, *108*, 4439−4450.

(31) (a) Barone, V.; Cossi, M. *J. Phys. Chem. A* **1998**, *102*, 1995−2001. (b) Cossi, M.; Barone, V. *J. Chem. Phys.* **2001**, *115*, 4708−4718. (c) Cossi, M.; Rega, N.; Scalmani, G.; Barone, V. *J. Comput. Chem.* **2003**, *24*, 669−681.

(32) Leonid, S. *Chemissian 1.7*; 2005−2010. Available at http://www.chemissian. com.

(33) Zhurko, D. A.; Zhurko, G. A. *ChemCraft 1.5;* Plimus: San Diego, CA. Available at http://www.chemcraftprog.com.

DOI: 10.1021/acs.inorgchem.5b01868
Inorg. Chem. 2015, 54, 10049−10057